Visual Discrimination of Membrane Domains in Live Cells by Widefield Microscopy

Claire E. Butler, Guy Wheeler, Jeremy Graham, and Kevin M. Tyler

Abstract Membrane dynamics is a fast-evolving field with the many new methods and probes being developed each year affording ever increased insights into how membranes behave in the laboratory. Typically, these developments are first tested in model membranes using high-cost, bespoke microscopes which often employ confocal and two-photon systems and which give little consideration to preservation of cellular integrity and homeostasis during experiments. This chapter addresses the clear need to rapidly apply and deploy this work into mainstream biological laboratories by development of economical, four-dimensional imaging on user-friendly low-cost systems using widefield optics and simultaneous capture of multiple fluorescent markers. Such systems are enabling biologists to consider the coordinated processes triggered from signalling platforms during cellular interaction with the environment. In this chapter, we describe the progress made to date and in particular we focus on the Laurdan family of fluorescent probes, which are being used to image whole cells and tissues using widefield epifluorescence microscopy and which can be usefully combined with simultaneous capture at longer wavelengths (yellow through far red) for imaging of cell morphology or for following expressed markers such as fluorescent adaptor proteins.

Keywords Laurdan · Membrane · Microdomains · Widefield microscopy

C.E. Butler, G. Wheeler, and K.M. Tyler (✉)
Biomedical Research Centre, Norwich Medical School, University of East Anglia, Norwich NR4 7TJ, England
e-mail: K.Tyler@uea.ac.uk

J. Graham
Cairn Research Ltd, Graveney Road, Faversham Kent ME13 8UP, UK

Y. Mély and G. Duportail (eds.), *Properties and Functions of Biological Membranes Investigated by Fluorescence Methods*, Springer Ser Fluoresc (2012), DOI 10.1007/4243_2012_47

Contents

1 Introduction

1.1 Plasma Membrane Composition

The plasma membrane is a dynamic interface between the internal cytoplasm and the extracellular milieu. As a lipid bilayer, it comprises a heterogeneous mix of lipid species including sterols, glycolipids and phospholipids. Phospholipids are defined by their hydrophilic "head" groups and by their hydrophobic "tails" which can vary in length and are generally either saturated or unsaturated fatty acids. Saturated fatty acid chains form long straight chains which pack closely excluding water (and some detergents) thereby reducing membrane hydration and fluidity. Conversely, unsaturated fatty acids contain double bonds which introduce kinks disrupting packing, increasing hydration and reducing membrane viscosity. There is believed to be a thermodynamically driven propensity for saturated fatty acids to coalesce to the exclusion of unsaturated fatty acids, giving rise to lateral organisation and regions or subcompartments of different biochemical composition with different biophysical characteristics [1].

Subcompartmentalisation of the plasma membrane has profound implications for cellular interaction with the environment, particularly with regard to cell signalling and cellular trafficking. Discrete regions within the plasma membrane, rich in saturated fatty acids and sterols which resist detergent treatment, are commonly referred to as lipid rafts, a term coined to graphically describe them in the context of, and as exceptions to, the fluid mosaic model [2]. GPI-linked (outer

leaflet) and acylated (inner leaflet) proteins, as well as sphingolipids, glycosphingolipids (including gangliosides) and sterols (typically cholesterol and/or ergosterol), are found to accumulate in these regions, which are usually <100 nm in size giving rise to the alternative name, microdomain. Surprisingly, transmembrane proteins including G-protein-coupled receptors (GPCRs) and ion channels are also associated in lipid rafts, typically this association is generally dependent on multiple acylations (typically palmitoylation)[3].

1.2 The Lipid Raft Debate

Two types of lipid rafts are widely described: detergent-resistant microdomains (DRMs) and caveolae. DRMs have been conceptualised as planar regions of the membrane, whereas caveolae are invaginations which require caveolin-1 to form [4]. Lipid rafts are also described as membrane attachment sites for cholera toxin which binds to ganglioside G_{M1} located in these regions allowing them to easily be localised [5].

There is however some debate over the very existence of lipid rafts, partly due to the large range in sizes reported for these regions, 10–200 nm, and their potentially transient nature [6]. The reported size variation may reflect the methods of analysis employed, particularly where cross-linkage of these domains as preparation for their observation may result in their translocation and fusion to form larger more stable structures [7]. Fixation of the plasma membrane generally alters its structure and integrity, thus creating a dilemma for the effective visualisation of microdomains. The detergent method of extraction is also problematic, as it leads to the production of large sheets of membrane, contamination and loss of components; however, it is still considered a useful tool, and a large number of lipid raft components were first isolated using this method [8].

The timescale of existence for lipid rafts is also still under discussion. Visualisation by FRET between acylated proteins and caveolin has suggested that they can be relatively stable structures [9], but others have described them as transient and only detectable in response to a stimulus [8]. Despite this controversy, a considerable number of studies have been published on the subject of lipid rafts. To date, it is widely accepted that eukaryotic plasma membranes are not simple liquids but two-dimensional nonideal liquids containing dynamic structures [7].

1.3 Membrane Domains and Membrane Polarisation: Cilia and Synapses, Infection and Immunity

Sterols and sphingolipids are almost exclusively associated with eukaryotic cells, and the peculiar association between sterols and sphingolipids in eukaryotes potentiates lateral segregation, subcompartmentalisation and sorting within contiguous membranes, upon which membrane trafficking and plasma membrane

polarisation are contingent [10]. More than 200 proteins have been associated with lipid rafts [11]; in some instances, cell surface receptors are permanently localised in these regions, with other receptors believed to relocate into lipid rafts after ligand binding [12, 13]. Although small, lipid rafts are thought to be able to fuse together upon binding of certain membrane receptors to create large signalling platforms and are therefore considered to be dynamic as well as transient [2]. Lipid rafts can also be stabilised by galectin lattices, structures formed by endogenous lectins which bind branches of the N-glycan domain on glycoproteins. These lattices likely increase the capacity for concerted actions such as signalling by concentrating receptors and signalling intermediates and also contribute to the regulation of the lifetime of lipid rafts [14]. Lipid rafts as signalling platforms have been described in GPCR signalling where such receptors are thought to cluster together within caveolae (described below) or to translocate upon activation to lipid rafts as summarised by [12].

Subcompartmentalisation of the plasma membrane in polarised cells into contiguous but discrete membrane domains with distinct biochemical compositions and which are large enough to be readily visualised is well documented. Even at a steady state, the apical and basolateral membranes of epithelial cells are known to have different constitutions reflecting membrane trafficking, which is believed to be dependent on lipid rafts. Similarly in ciliated cells, the ciliary membranes have a distinct biochemical composition from the somatic regions of the plasmalemma, and this may reflect not only trafficking but sorting at the ciliary junction and the propensity of lipid rafts to accumulate in membrane protrusions [15, 16]. For budding yeast, lipid rafts are fundamentally associated with apical sorting for polarised growth and cell-cell interaction during mating [17]. In other cell-cell and cell-pathogen interactions, the plasma membranes also become effectively polarised at the contact site or synapse, and a discrete functional domain is formed in response to contact with other cells or during contact with a pathogen be it viral (e.g. dengue and HIV) [18, 19], bacterial (e.g. Shigella and Campylobacter) [20] or parasitic (e.g. malaria and *Trypanosoma cruzi*) [21, 22]. Common to all of these interactions is the ligation of raft-associated surface receptors which are commonly glycoproteins or glycolipids and the requirement for this interaction to generate signalling in order to effect cellular function – supporting the prevailing view of a key role for lipid raft formation in environmental sensing by formation of signalling platforms [2]. With this in mind, increasing the accessibility of membrane imaging will help drive forward the field of pathogen-cell interaction.

2 Lipid Domain-Binding Probes

2.1 Cholera Toxin

A variety of molecular markers have been produced for the visualisation and functional analysis of lipid rafts. Cholera toxin B (CtxB) from *Vibrio cholerae* is known to bind the ganglioside G_{M1} which generally localises to microdomains.

Fluorescent fusions of CtxB can therefore be used to image the interaction between CtxB and G_{M1} specifically [23], for example, G_{M1} localisation and patching have been used to identify pathways for MHC endocytosis [24]. Although this association is a widely used method for identifying lipid rafts, there are some limitations; G_{M1} is also sometimes found outside of the lipid raft fraction, and the binding of CtxB and G_{M1} may also result in the clustering of sphingolipids [25, 26]. CtxB is capable of simultaneously binding five separate G_{M1} molecules which may be located in five different lipid rafts, consequently dynamic domains will be stabilised, and there is some evidence to suggest that CtxB can cross-link other molecules such as glycoproteins resulting in a loss of specificity of the detection. CtxB can also be conjugated to quantum dots for live cell imaging as well as observing the progression between generations [27]. Quantum dots are semiconductor nanocrystals which can be used for a wide range of applications but usually in conjunction with confocal microscopy [28].

2.2 *Fluorescent Sphingolipids and Sphingolipid-Binding Proteins*

Sphingolipids are another component of lipid rafts, and the fluorescent sphingolipid-binding domain (SPD) appears to interact with cholesterol, sphingomyelin and glycosphingolipids enabling live cell imaging of the endocytic pathways of these lipid raft components [29, 30]. SPD is derived from amyloid β-peptide and interacts with the glycophospholipid head groups. Sphingomyelins (a species of sphingolipid) are around 50 % more prevalent in lipid rafts than in the rest of the membrane [31] making them an ideal target for fluorescent probes. Lysenin, a toxin which has an affinity for sphingomyelin-rich domains [32], has shown a plasma membrane distribution separate from that of G_{M1} microdomains [33] suggesting that there may be a separate genre of sphingomyelin-associated lipid rafts. Sphingomyelin synthase, which catalyses its synthesis from ceramide and phosphotidylcholine, is thought to regulate clustering of the product [34] and so may play a role in one or other genre formation. Lysenin is more specific than other probes in that it only recognises sphingomyelin and no other sphingolipids; thus, potentially lysenin may be a candidate to specifically study lipid rafts [35]. The main problem with lysenin as an imaging tool is that it is cytotoxic in most cells, and thus, it was necessary to develop a truncated form without the cytotoxic N terminus [36] before it could be used reliably.

2.3 *Fluorescently Labelled Cholesterol*

Cholesterol appears 50 % more concentrated in lipid rafts than in the plasma membrane [31] and therefore may be used as a microdomain marker. Polyene antibiotics such as filipin bind free cholesterol at a 1:1 stoichiometry at the cell

surface, resulting in emission of light in the ultraviolet range of the spectrum [37], and thus could be used as a fluorescent cholesterol marker. Filipin can also diffuse across the membrane and incorporate into the inner leaflet providing additional structural information as well as details about the Golgi membrane [38]. Despite its widespread usage as a lipid raft marker, filipin does not necessarily discriminate between lipid rafts, and the cholesterol at the rest of the cell surface and accumulation of filipin over time has proven cytotoxic; thus, alternative cholesterol probes have been developed.

Perfingolysin O is another cholesterol-binding cytolysin which can bind large cholesterol structures and therefore detect cholesterol-enriched domains. A perfringolysin O domain D4 fusion protein has also been shown to bind cholesterol specifically localised in lipid rafts [39] and has revealed the presence of lipid rafts on the inner leaflet of the plasma membrane [40].

Dehydroergosterol (DHE) is a naturally occurring cholesterol analogue which differs from cholesterol only in possessing two double bonds and an extra methyl group and is able to incorporate into the cell membrane at a concentration of up to 85% before any cytotoxic effects are observed [41]. Absorption and emission spectra are in the UV region but can be imaged with epifluorescence after some minor modifications [42]. DHE can also be used to visualise the sterol distribution in living cells although this method does not exhibit a particular affinity for G_{M1} discernable microdomains [43] and may not behave functionally as cholesterol.

Polyethylene glycol-derived cholesterol ether (PEG-Chol) has a high affinity for cholesterol-rich domains, and addition of a fluorescent ester (e.g. fluorescein) has led to the production of a lipid raft-specific probe (fPEG-chol). Its lack of cytotoxity meant that it was initially used to help disperse otherwise insoluble antibiotics [44]. Its size prevents movement to the inner leaflet of the membrane, but it is still a useful tool to monitor reorganisation of lipid rafts at the cell surface [45], exhibiting a similar distribution to that of filipin and being internalised along with lipid raft components [46].

The enrichment of sphingolipids in lipid raft regions also provides the opportunity for labelling sphingolipids and their analogues with BODIPY (boron dipyrromethane [(4,4-difluoro-4,7-dimethyl-4-bora-3a,4a,diaza-s-indacene)]) to investigate structure and function. BODIPY-labelled sphingolipids have interesting spectral properties and show a shift in emission spectra from green to red at increased molar densities [47]. Both BODIPY-Cer in vitro and BODIPY-LacCer in live cells can therefore be used to differentiate specific regions of the cell membrane by wavelength. Furthermore, BODIPY can be conjugated to cholesterol in a manner that does not inhibit normal cholesterol function and allows its partitioning into regions of high lipid order [48] and also to sphingomyelin, where it has been observed incorporating into lipid rafts in an endogenous sphingomyelin-dependent manner [49]. A derivative, BODIPY-*D-erythro*-LacCer, has also shown that sphingolipids can be induced to redistribute into specific microdomains on the plasma membrane in response to CtxB.

Sphingolipid positioning within the plasma membrane is controlled by palmitoylation, a process affecting membrane microlocalisation that is regulated during sphingolipid biosynthesis by a family of aspartate-histidine-histidine-cysteine

palymitoyl transferases (DHHCs). Labelling DHHC's allows the monitoring of their positions in the cell membrane in response to different stimuli, and the live imaging of DHHC recycling to and from the plasma membrane has been recently described [50].

3 Adaptor Proteins

3.1 Caveolin

A number of adaptor proteins are found to cluster in lipid-rich microdomains, and fluorescent fusion proteins have become widespread in live cell imaging for caveolin and flotillin. Caveolae, which have been mentioned previously, are distinct cell surface membrane invaginations associated with endocytosis (reviewed by [51]). These structures are rich in cholesterol, and indeed, the presence of cholesterol is required for efficient formation of these structures, leading to them being proposed as a form of lipid raft. Each caveola contains clusters of GPI-linked proteins and acylated proteins packed to a density of some 30,000 molecules per square micrometre [52].

As well as cholesterol, the formation of caveolae also requires the presence of a scaffolding protein called caveolin which coats the cytoplasmic surface of the invagination [53]. There are three subtypes of caveolin with caveolin-1 and caveolin-2 the most abundant, being present in a wide range of cell types especially epithelial lines [54], whereas caveolin-3 is confined to muscle cells [55]. All three subtypes appear to exhibit similar functions in cell signalling, lipid raft formation, trafficking and possibly heterotrimeric G-protein signalling [56] although of these, caveolin-2 has proven non-essential for caveolae formation.

Fusion proteins for all three isomers of caveolin have been used to elucidate the structure of caveolae and their function as well as the mechanism of caveolin transport to and from the plasma membrane [57]. In fact, the use of fusion proteins has been integral to all the major steps forward in caveolin protein-protein understanding, suggesting such roles as a negative-signalling molecule, the base of a signalling platform and antigen presentation.

3.2 Flotillin

Another protein which is thought to be lipid raft associated is flotillin-1 (flot1) which is sometimes referred to as reggie-2. This protein is important in an endocytic pathway separate to that of the caveolae [58]. Flotillin-based structures are uncoated invaginations in the cell surface membrane that are dependent on the coassembly of flot1 and 2 to promote membrane curvature [59]. Internalisation in this pathway is regulated by the src family kinase, fyn [60], which is considered to

be involved in endocytosis of GPI-linked signalling molecules [61]. Again, its fluorescent fusion proteins have been integral in the above microscopy studies, also showing both caveolin and flotillin to be found only in specific subsets of cells and in their own types of membrane microdomains.

3.3 GPI-Linked Proteins

An alternative approach may be to use fluorescent protein-coupled GPI-adaptor proteins (GPI-APs) which would insert directly into the lipid raft, which, as previously stated, are rich in GPI-anchored proteins. However, the size of these molecules may cause perturbation within such a small system, and expression of these fluorescent proteins may also lead to their fluorescence in their biosynthetic pathway.

4 Environment Sensitive Probes

4.1 Laurdan

The fluorescent probe Laurdan (6-dodecanyl-2-dimethylaminonaphthalene) has been used to study the lateral organisation of membrane domains since it was first synthesised in 1979 [62], due to its ability to incorporate into the membrane with an even distribution, without detectably altering the physiology of the cell and without being altered by cell surface interactions such as the binding of lipoproteins. The Laurdan dipole aligns with the phospholipid bilayer between the lipid head groups and the first carbon atom of the acyl chains, and its emission spectra changes depending upon the fluid state of the surrounding lipid chains [63]. In a more fluid membrane domain, Laurdan fluoresces with greater intensity at green wavelengths, with a maximum centred around 490 nm. This shifts to 440 nm and a blue fluorescence, in more ordered membrane regions. A method for the ratiometric analysis of Laurdan fluorescence, the generalised polarisation (GP), was developed to help identify the fluid order of Laurdan-stained membranes [64, 65], giving a range for GP values between −1.0 and +1.0; the more positive the GP value, the more ordered the membrane.

Laurdan has been extensively used for studying membrane dynamics, with over 300 reports in the literature. However, the vast majority of these use either fluorescence spectrophotometry [66, 67], evaluating the GP of entire preparations, or two-photon [68] and confocal microscopy [69]. Recently, confocal microscopy has also been used to explore the liquid order of a zebra fish embryo initiating the development of novel whole organism techniques [70]. Alternatively, many studies have utilised artificially synthesised unilammelar vesicles or membrane extracts from biological systems. It is only in the last few years that reports have been published using Laurdan fluorescence with epifluorescence microscopy on live cells [71, 72].

The reasons for using microscopy rather than spectrophotometry have been described previously [73]. Two-photon microscopy is able to minimise the rapid photobleaching that Laurdan is susceptible to, particularly under widefield fluorescence microscopy; however, the cost of the system may render it inaccessible. Ultimately, the bleaching effect of Laurdan under widefield microscopy can be overcome [71, 74]. Taken together, such studies demonstrate clearly that the GP is higher for surface membranes compared to intracellular membranes and demonstrate the utility of their systems through seeing the expected shift of emission spectra and GP values in increasingly fluid membranes.

The key to using Laurdan-stained live cells under widefield conditions is to be able to utilise other markers and fluorescent proteins. This affords the ability to identify interactions and monitor responses and to co-localise membrane markers with membrane phases and gauge the cellular response whilst monitoring the extent of membrane disruption in cases such as cholesterol depletion. Widefield Laurdan microscopy has been used to demonstrate that temperature can directly affect membrane fluidity but that living cells (in this case the ciliated protozoan *Paramecium*) can respond to changing environmental conditions by rapid adaption – restoring fluidity to a cooled membrane [75]. Further, Sitrin and colleagues have reported the utility of Laurdan using widefield microscopy, with a time-lapse assay of neutrophil migration [76]. Their widefield setup used an emission splitter to isolate the emission spectra of Laurdan for GP analysis. They showed over a 10-min time course with 10-s intervals that the migration tip of the neutrophils, the uropod, had consistently higher GP values compared to the rest of the cell but that this was a dynamic system, with high-GP regions within the uropod-shifting position even between the 10-s time points. They also showed that application of the cholesterol depletory MβCD, which therefore lowers GP, marginally slowed the speed of the neutrophil migration but also reduced its ability to migrate towards chemotactic signals. These studies demonstrate utility of widefield Laurdan microscopy in assessing membrane dynamics in live cells distinct and from spectrophotometry or the two-photon system; photobleaching can be minimised because epifluorescent sources can be of low intensity compared with confocal and exposure times can be low when combined with a high-sensitivity CCD. Whilst the latter study reported that receptors known to be involved in cell movement pathways localised to higher GP regions, they were unable to co-localise structures using fluorescent markers or to observe the cell directly using condenser-based techniques such as phase-contrast or DIC microscopy. Weber and colleagues combined widefield Laurdan microscopy with fluorescence anisotropic microscopy and total internal reflection (TIR) microscopy using a flexible setup that allowed them to look at membrane stiffness of the plasma membrane in living cells and compare it to internal membranes whilst varying temperature and cholesterol content [74]. This flexible setup afforded the ability to image cells at long wavelength but not to capture and compare simultaneously and in real time.

Laurdan microscopy for live imaging of cultured cells can be set up straightforwardly at modest cost on an inverted fluorescent microscope using the setup described in Fig. 1. Key to the system is the triple emission beam splitter which

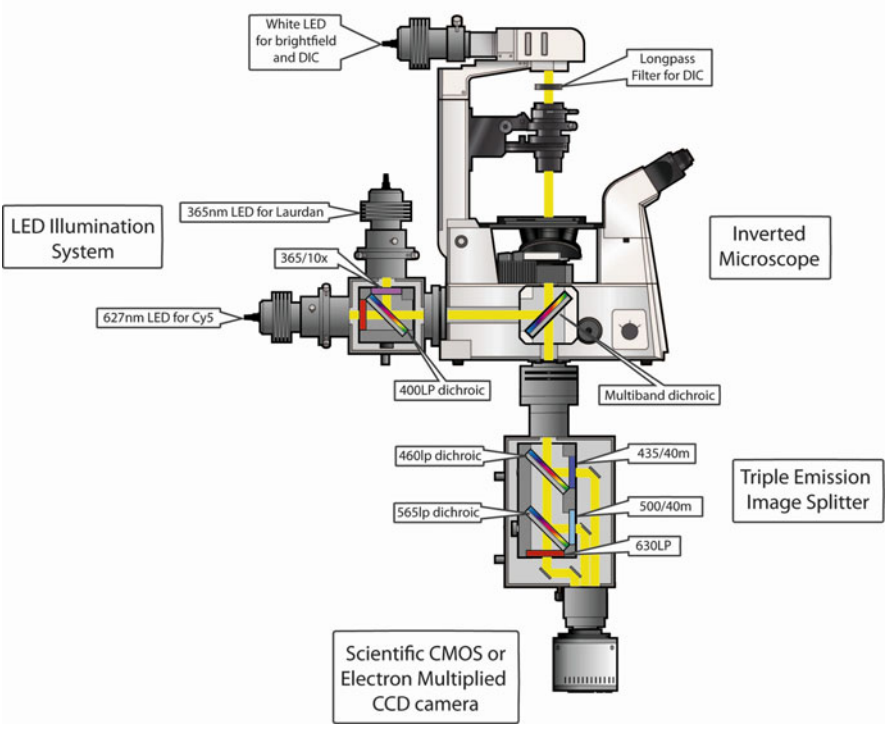

Fig. 1 Widefield Laurdan microscopy setup. Figure shows an experimental setup for imaging Laurdan simultaneously with (*1*) Cy5 or other red/far-red fluorophore, (*2*) infrared DIC or other transmitted light technique using red or infrared illumination, and (*3*) both (*1*) and (*2*), alternating in time. The configuration consists of a research-grade inverted fluorescence microscope with a high numerical aperture objective lens and an image splitter capable of separating the emission pathway into three spectrally distinct channels using either a splitter device (e.g. Cairn Research TripleSplit, Photometrics QuadView) or three independent cameras and appropriate beam-splitting optics (e.g. Cairn Research TriCam). In order to ensure high stability and minimise photobleaching, a rapidly modulated LED-based light source is preferred for both fluorescence and transmitted light illumination (Available from Cairn Research, CoolLED, 89 North, Lumencor, Prior Scientific). A back-illuminated electron-multiplied camera will give maximum sensitivity allowing illumination levels to be minimised; alternatively an SCMOS camera might be preferred to give higher resolution and a larger field of view (suitable cameras available from Andor, Photomterics, Hamamatsu, PCO). For truly simultaneous imaging and to avoid vibration or registration problems, the microscope dichroic must be multiband so that it can remain in the lightpath at all times (typically a Quad Sedat 4-band dichroic). The excitation and emission filters and dichroic mirrors need to be carefully selected to fit with this multiband device (Available from Chroma Corporation, Semrock, Omega); suggested wavelengths and bandwidths are indicated in the diagram. In protocol (*1*), the 365-nm and 627-nm LEDs on the epifluorescence port should be triggered to be on whenever the camera is exposing. In protocol (*2*), the 365-nm fluorescence and white-transmitted LED should be triggered with the camera. In protocol (*3*), the 365-nm LED is triggered every frame, and the 627-nm and white LED are triggered on alternating frames. The "red" emission channel should then be demultiplexed after acquisition

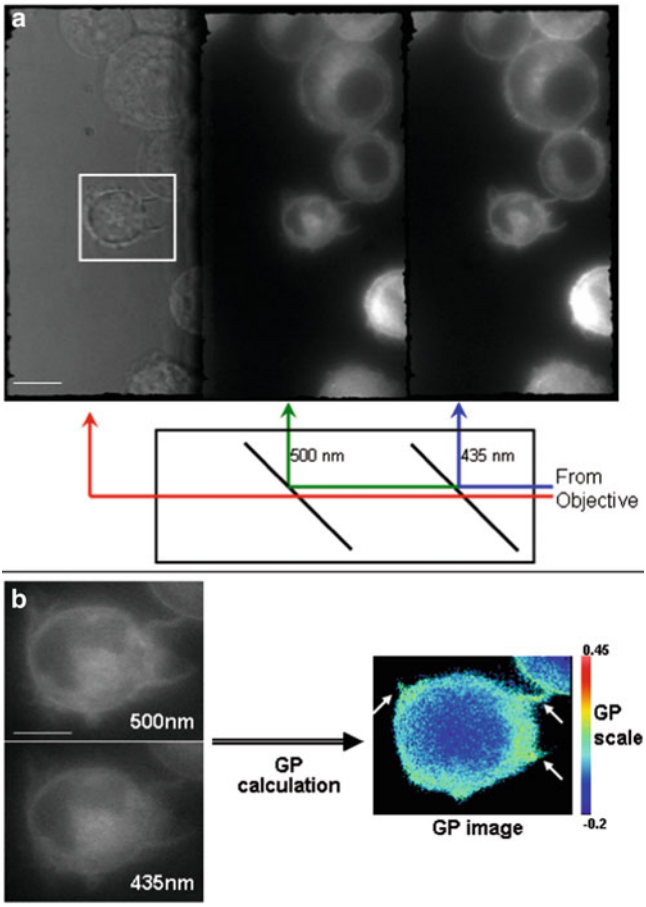

Fig. 2 Widefield Laurdan microscopy. Representation of the Optosplit III block with dichroic mirror set up for Laurdan staining. The two dichroic mirrors separate the fluorescence emission of the Laurdan-stained cells into the blue (435 nm) and green (500 nm) wavelengths, with a third channel showing light from the red end of the spectrum (N500 nm) (**a**). Calculation of the generalised polarisation of the cell outlined in (**a**) showing fluorescence at the blue and green wavelengths (**b**) and the GP image calculated from these. The range of values represented on the pseudo-coloured GP image is shown as a colourimetric scale to the right of the GP image. Filopodia are highlighted with *arrows* in the GP image. Scale bars = 10 μm (**a**) and 5 μm (**b**)

allows for acquisition of distinct images from three different wavelengths in parallel, in real time (Fig. 2). This allows for biological phenomena (such as filipodia formation, shown here) and processes to be followed. Laurdan technology can also be combined with fluorescent protein imaging to study the interaction of protein-coated microparticles with the cell surface prior to internalisation (Fig. 3). Laurdan emission is restricted to visible wavelengths in the blue/green area of the spectrum, and thus, by imaging with fluorescent markers or a

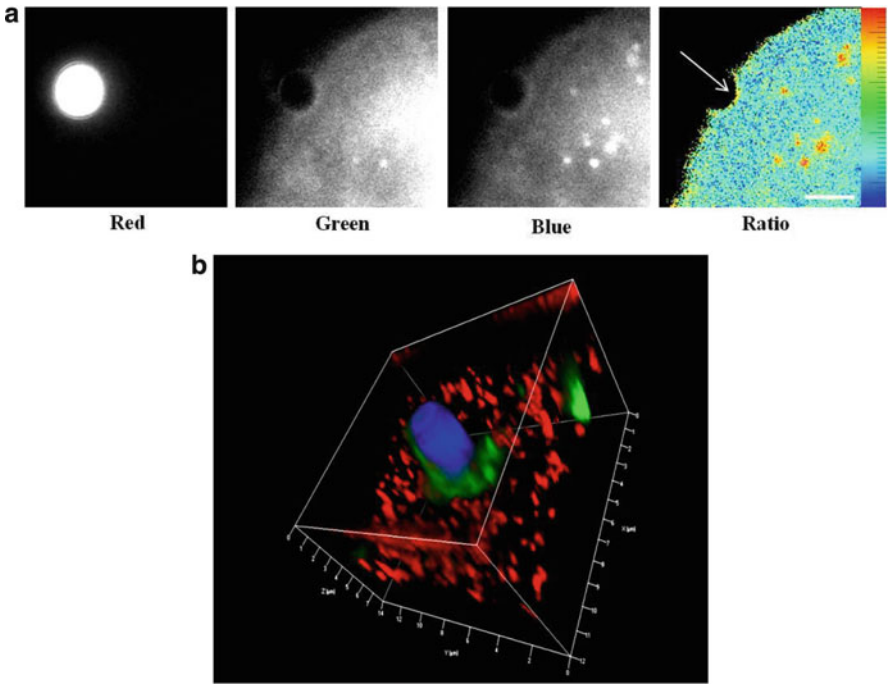

Fig. 3 Coated beads which bind to glycosylated moeities on the cell surface induce high lipid order and recruit raft markers such as caveolin to the bound area of the plasma membrane. Triplesplit images of a trans-sialidase-coated bead (*red*) and *green* and *blue* images of a Laurdan-labelled cell (**a**), GP analysis (*ratio*) shows a region more highly ordered at the area of bead attachment (*arrow*). Scale bar = 4 μm. Early endosome (*red*) and cav1 (*green*) immunolabelling of MDCK cells show an accumulation of cav1 at the bead (*blue*)-cell interface. Images were taken with a Zeiss Axioplan2 microscope and deconvolved before reconstructing into a 3D representation using Axiovision software (**b**)

transmitted light in the red/far red of the spectrum, high-resolution imaging of the cell or fluorescent cellular markers may be utilised to identify regions of interest. Having identified the region of interest, the GP of that area can be quantified directly (Fig. 4). In addition, it is possible to facilitate discrimination of areas of distinct GP by setting thresholds and masking areas outside the threshold as in the case of a living protozoan flagellum shown here as distinct from the rest of the plasmalemma (Fig. 5).

Another benefit to using a widefield setup may be the reduction of the photoselection effect. This arises from the way Laurdan molecules align parallel to the lipid chains in the membrane and that the light used for its excitation in confocal and two-photon microscopy is polarised giving rise to the strongest excitation in those molecules parallel to the plane of the light [73]. The irregular shape of cells, with regions inevitably in many different orientations relative to the plane of excitation, results in an uneven excitation of Laurdan molecules, skewing

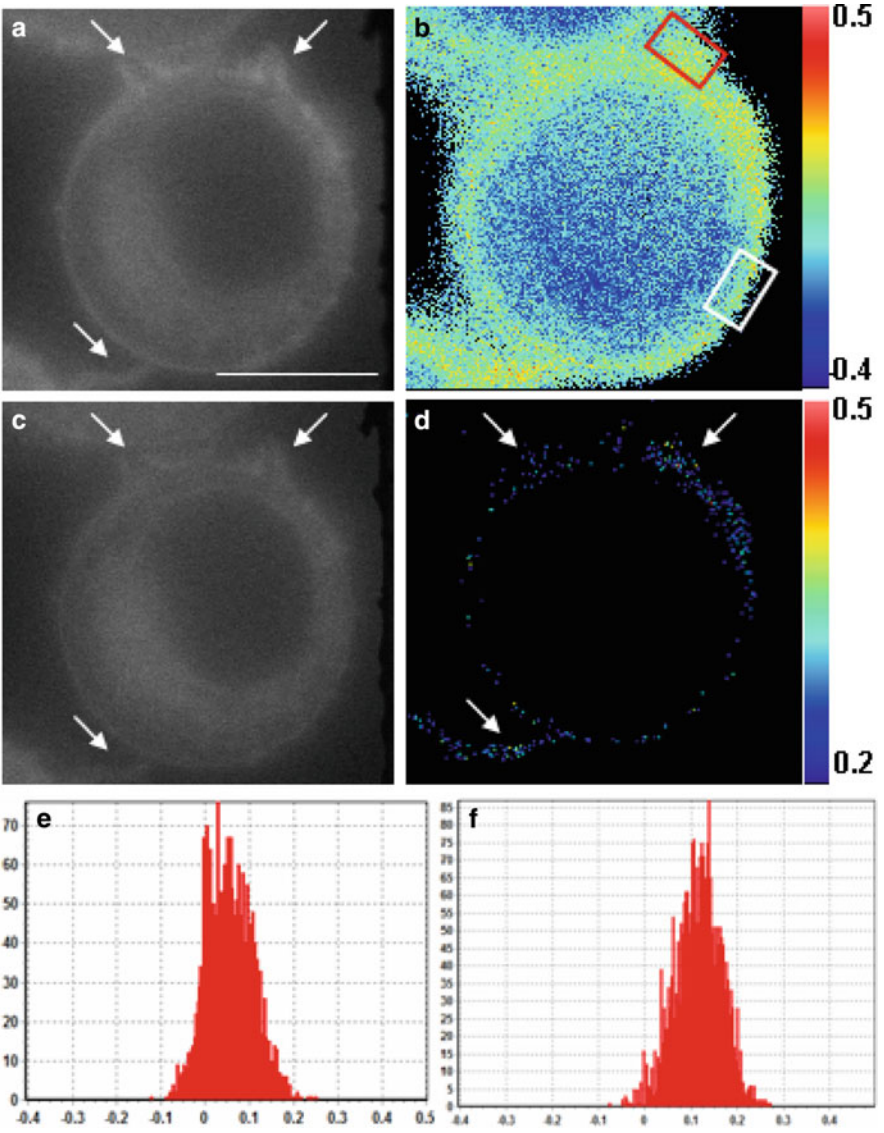

Fig. 4 Isolation of discrete high and low generalised polarisation regions within a RAW264.7 cell membrane. Filopodia are highlighted (*arrows*). Fluorescence of Laurdan stained. RAW264.7 cell in the blue (**a**) and green (**c**) wavelengths. (**b**) GP of the cell showing the range of the cell's calculated GP values. Regions of high (*red box*) and low (*white box*) membrane order are shown. (**d**) GP image showing only those pixels with a GP of 0.2 or more. The regions around the filopodia appear more ordered. GP histograms (x-axis = GP value, y-axis = number of pixels) of the high- (**e**) and low- (**f**) order regions from (**b**). Scale bar = 5 μm

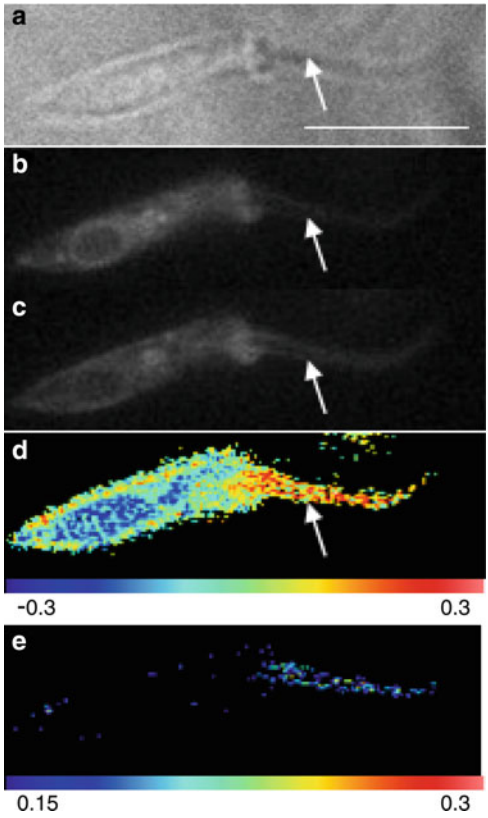

Fig. 5 Laurdan staining of *Trypanosoma rangeli*. Far-red illuminated brightfield (**a**) and fluorescent images (**b** and **c**) of a Laurdan-stained *T. rangeli* using the triplesplit widefield microscope. GP analysis (**d**) shows the more highly ordered flagellum (*arrow*) when compared to the rest of the cellular membrane. Exclusion of low-GP pixels (**e**) demonstrates the greater number of high-GP pixels in the flagellum. Scale bar = 4 μm

the GP measurements. This effect is particularly pronounced in more ordered regions, where the Laurdan molecule is even more rigidly aligned with the membrane. Although direct analysis of the magnitude of the photoselection effect and methods for its mitigation are not yet published, it is believed that non-polarised light sources such as those used in widefield setups reduce this artefact markedly [71, 77].

4.2 C-Laurdan

Despite its use in these studies, Laurdan is still limited as a tool for studying membrane dynamics in living cells due to its rapid photobleaching and hydrophobic nature. It is not readily soluble in water, but instead a solute such as DMSO or methanol must be used, which may itself have an effect on the target cell [15]. An improvement on Laurdan has recently been synthesised [78]: 6-dodecanoyl-2-[*N*-methyl-*N*-(carboxymethyl)amino]naphthalene, or C-Laurdan. This has proven to be more photostable and to have higher water stability arising from the

substitution of one of Laurdan's methyl groups with a carboxylic group. The improvement of C-Laurdan over Laurdan in this regard has already been shown in two-photon microscopy (e.g. [79] with potentially greater benefits in widefield microscopy, allowing prolonged excitation and its application in a more neutral vehicle buffer).

In spite of the improvement offered by C-Laurdan, GP imaging of membrane domains remains far from optimal. The need for the highest possible resolution GP imaging in combination with the simultaneous imaging of the whole cell and additional markers of cellular behaviours (such as cell signalling) in order to obtain a maximum amount of biological information remains to be addressed. It is not clear to what extent such images can be subjected to standard deconvolution software to increase image quality and clarity, and this is an area which should be considered in the future. Further, the monopolisation of a broad (blue/green) area of the spectrum required by Laurdan significantly limits the scope for the number and types of processes and cellular behaviours that can currently be simultaneously imaged, typically restricting investigators to simply mapping the GP image onto a simultaneously captured image of the cell, or to follow just one or two additional cellular markers at the (red) end of the spectrum.

4.3 Di-4-ANEPPDHQ

Di-4-ANEPPDHQ is an environmentally sensitive styryl dye that can also be used to differentiate between liquid-ordered phases and liquid-disordered phases both in GUV's and polarised neutrophil membranes [80, 81]. Similar to Laurdan, di-4-ANEPPDHQ can indicate lipid packing without being affected by inserted peptides, [82] and both can be used in lower resolution techniques [83]. It incorporates into the membrane in a different manner to Laurdan, aligning with the acyl heads deeper into the membrane. Its two positive charges also confer a lesser ability to flip between the inner and outer leaflets, but its solubility in water does make it a more useful tool for studying live cells and thus in the future could be adapted for use with a widefield microscope.

5 FRET/FLIM

5.1 FRET

The development of Förster resonance energy transfer (FRET) has enabled the imaging of physical processes occurring at the cell surface in real time and to this end is a commonly used technique. Excitation of a fluorescent molecule occurs upon absorption of a photon leading to one of its electrons being promoted to a

higher energy level. When this electron returns to its lower energy state, energy is released in the form of light. FRET essentially is the nonradioactive transfer of this energy to a nearby acceptor molecule instead of its loss by fluorescence. The extent of FRET is dependent primarily on three factors: the spectral overlap of the donor and acceptor fluorophores, their closeness (i.e. 1–10 nm apart for the ratio between the donor and acceptor fluorescence levels to be measured) and their dipole-dipole interaction. Initial utilisation of FRET was limited to purification of specific molecules and their reintroduction, the methodology being destructive and requiring microinjection. The development of green fluorescent protein (GFP) as a tool led to a non-invasive protocol for the introduction of the tagged molecules by transfection. Since the pioneering introduction of GFP, many other fluorescent analogues have been extracted, and the current fluorescent proteins of choice for FRET are YFP (yellow) and CFP (cyan), first seen in conjugation with retinoic, steroid receptor coactivator-1 and peroxisome proliferator-activated receptor-binding protein [84]. Although widely used, both YFP and CFP are pH sensitive [85, 86], thus restricting their use to biological processes which do not alter cellular pH. Recent work has seen the development of pH-stable versions of YFP, Venus [87] and Citrine [88] which should therefore prove more exploitable in living cells.

Similar to FRET, homo-FRET relies on two fluorophores being less than 10 nm apart for the exchange of energy; however, both fluorophores are the same, and therefore, interaction cannot be monitored by changes in fluorescence emission. Nevertheless, processes leading to close approach, for example, oligomerisation, can be followed using anisotropy measurements that reflect changes in fluorophore polarisation, both due to energy transfer and changes in molecular rotation. The use of these tools for studying lipid rafts has been neatly reviewed by [89]. The ability to detect the rotation of specific lipids within the membrane gives a general idea of the level of fluidity in specific regions of the membrane and therefore the level of lipid order. Similarly, this microscopy technique has also been used to show that BODIPY-cholesterol arranges itself into the membrane and into specific regions of higher order [90]. In addition to determining orientation, anisotropy can also be used to shed light on protein clustering: by calculating the rate of homo-transfer, the distance between fluorophores can be determined, and the number of molecules per cluster elucidated. The size of the protein clusters in lipid rafts and the spatial distribution has also been determined using anisotropy techniques [91]. The clustering of GPI-AP's into regions of the plasma membrane of approximately 4–5 nm has also been described using anisotropy [92]. All of these studies, however, are used with either confocal or two-photon microscopy, so an important question for the field is as follows: can FRET be used with widefield microscopes? Indeed it can; however, the resultant images can be affected by a significant amount of noise, blurring the signal from excited fluorophores. This additional noise can now be removed using 3D-FRET reconstruction and additional photobleaching correction [93] thus cost-effectively improving accessibility of this technique.

5.2 FLIM

FRET microscopy can also be combined with fluorescence lifetime imaging microscopy (FLIM) to monitor signalling across the whole plasma membrane [94]. There are two types of FLIM (time domain and frequency domain), but for the purposes of this chapter, we will discuss only the frequency-domain method which is best suited for widefield microscopy. When a fluorophore becomes excited, the transition from the excited state to the ground state occurs over a given average decay time that can be measured using FLIM techniques. FLIM in recent years has been employed in the study of lipid rafts which has been reviewed in [95]. Although the majority of these studies have been done using GUV's and other controlled model membrane systems to reduce the complex lipid-protein interactions, FLIM for live cells was demonstrated by Owen and co-workers in 2006 using di-4-ANEPPDHQ and normalising their system with unilamellar vesicles. Here, the FLIM contrast gave good resolution of regions of high lipid order indicative of lipid rafts, especially when concentrated in membrane protrusions [96]. To date, all FLIM work on lipid rafts has been done using confocal or two-photon systems, but widefield FLIM systems are now commercially available, and so it may only be a matter of time before this type of imaging is applied to the study of lipid rafts.

6 Conclusions

Membrane dynamics is a fast-evolving field with the many new methods and probes being developed each year affording ever increased insights into how membranes behave in the laboratory. However, the major limitations of these techniques lie typically with the high cost of bespoke microscopes which often employ confocal and two-photon systems and which give little consideration to preservation of cellular integrity and homeostasis during experiments. There is a clear need to rapidly apply and deploy this work into mainstream biological laboratories by development of economical, 4-dimensional imaging on user-friendly systems using widefield optics and simultaneous capture of multiple fluorescent markers. Such systems should enable biologists to consider the coordinated processes triggered from signalling platforms during cellular interaction with the environment. A plethora of microscopic methods and labelling molecules have been described, but many have some disadvantages for use in live cells or are confined in their use to very small regions of the cell membrane. The Laurdan family of fluorescent probes, however, can be used to image whole cells and tissues and can be combined with longer wavelength (yellow through far red) fluorescent adaptor proteins. Although, developed for use in confocal and two-photon systems, application to widefield-based investigation is now established and should facilitate future investigations seeking to relate modulation of plasma membrane dynamics to resultant change in cellular behaviour.

Acknowledgements We thank Dr. Paul Thomas at The Wellcome Laboratory for cell imaging for critical reading of the manuscript and advice and insight along the way and Rosanna Davies for her tremendous illustrative skills in producing the drawing of our widefield Laurdan microscopy setup.

References

1. Lingwood D, Simons K (2010) Lipid rafts as a membrane-organizing principle. Science 327 (5961):46–50
2. Simons K, Ikonen E (1997) Functional rafts in cell membranes. Nature 387(6633):569–572
3. Levental I et al (2010) Palmitoylation regulates raft affinity for the majority of integral raft proteins. Proc Natl Acad Sci U S A 107(51):22050–22054
4. Lisanti MP, Tang ZL, Sargiacomo M (1993) Caveolin forms a hetero-oligomeric protein complex that interacts with an apical GPI-linked protein: implications for the biogenesis of caveolae. J Cell Biol 123(3):595–604
5. Badizadegan K et al (2004) Trafficking of cholera toxin-ganglioside GM1 complex into Golgi and induction of toxicity depend on actin cytoskeleton. Am J Physiol Cell Physiol 287(5): C1453–C1462
6. Pike LJ (2006) Rafts defined: a report on the Keystone symposium on lipid rafts and cell function. J Lipid Res 47(7):1597–1598
7. Kusumi A, Suzuki K (2005) Toward understanding the dynamics of membrane-raft-based molecular interactions. Biochim Biophys Acta 1746(3):234–251
8. Lai EC (2003) Lipid rafts make for slippery platforms. J Cell Biol 162(3):365–370
9. Zacharias DA (2002) Sticky caveats in an otherwise glowing report: oligomerizing fluorescent proteins and their use in cell biology. Sci STKE 2002(131):pe23
10. Simons K, Sampaio JL (2011) Membrane organization and lipid rafts. Cold Spring Harb Perspect Biol 3(10):a004697
11. Lang T (2007) SNARE proteins and 'membrane rafts'. J Physiol 585(Pt 3):693–698
12. Insel PA et al (2005) Compartmentation of G-protein-coupled receptors and their signalling components in lipid rafts and caveolae. Biochem Soc Trans 33(Pt 5):1131–1134
13. Zhang Y et al (2009) Ceramide-enriched membrane domains–structure and function. Biochim Biophys Acta 1788(1):178–183
14. Lajoie P et al (2009) Caveolin-1 regulation of dynamin-dependent, raft-mediated endocytosis of cholera toxin-B sub-unit occurs independently of caveolae. J Cell Mol Med 13 (9B):3218–3225
15. Tyler KM et al (2009) Flagellar membrane localization via association with lipid rafts. J Cell Sci 122(Pt 6):859–866
16. Vieira OV et al (2006) FAPP2, cilium formation, and compartmentalization of the apical membrane in polarized Madin-Darby canine kidney (MDCK) cells. Proc Natl Acad Sci U S A 103(49):18556–18561
17. Bagnat M, Simons K (2002) Cell surface polarization during yeast mating. Proc Natl Acad Sci U S A 99(22):14183–14188
18. Reyes-Del Valle J et al (2005) Heat shock protein 90 and heat shock protein 70 are components of dengue virus receptor complex in human cells. J Virol 79(8):4557–4567
19. Liu NQ et al (2002) Human immunodeficiency virus type 1 enters brain microvascular endothelia by macropinocytosis dependent on lipid rafts and the mitogen-activated protein kinase signaling pathway. J Virol 76(13):6689–6700
20. Watson RO, Galan JE (2008) Campylobacter jejuni survives within epithelial cells by avoiding delivery to lysosomes. PLoS Pathog 4(1):e14

21. Silvie O et al (2006) Cholesterol contributes to the organization of tetraspanin-enriched microdomains and to CD81-dependent infection by malaria sporozoites. J Cell Sci 119(Pt 10):1992–2002
22. Fernandes MC et al (2007) Novel strategy in *Trypanosoma cruzi* cell invasion: implication of cholesterol and host cell microdomains. Int J Parasitol 37(13):1431–1441
23. Kuziemko GM, Stroh M, Stevens RC (1996) Cholera toxin binding affinity and specificity for gangliosides determined by surface plasmon resonance. Biochemistry 35(20):6375–6384
24. Knorr R, Karacsonyi C, Lindner R (2009) Endocytosis of MHC molecules by distinct membrane rafts. J Cell Sci 122(Pt 10):1584–1594
25. Antes P, Schwarzmann G, Sandhoff K (1992) Detection of protein mediated glycosphingolipid clustering by the use of resonance energy transfer between fluorescent labelled lipids. A method established by applying the system ganglioside GM1 and cholera toxin B subunit. Chem Phys Lipids 62(3):269–280
26. Janes PW, Ley SC, Magee AI (1999) Aggregation of lipid rafts accompanies signaling via the T cell antigen receptor. J Cell Biol 147(2):447–461
27. Chakraborty SK et al (2007) Cholera toxin B conjugated quantum dots for live cell labeling. Nano Lett 7(9):2618–2626
28. Rivera EM et al (2011) Imaging heterostructured quantum dots in cultured cells with epifluorescence and transmission electron microscopy. Proc SPIE 7909:79090N
29. Steinert S et al (2008) A fluorescent glycolipid-binding peptide probe traces cholesterol dependent microdomain-derived trafficking pathways. PLoS One 3(8):e2933
30. Hebbar S et al (2008) A fluorescent sphingolipid binding domain peptide probe interacts with sphingolipids and cholesterol-dependent raft domains. J Lipid Res 49(5):1077–1089
31. Pike LJ et al (2002) Lipid rafts are enriched in arachidonic acid and plasmenylethanolamine and their composition is independent of caveolin-1 expression: a quantitative electrospray ionization/mass spectrometric analysis. Biochemistry 41(6):2075–2088
32. Kiyokawa E et al (2004) Recognition of sphingomyelin by lysenin and lysenin-related proteins. Biochemistry 43(30):9766–9773
33. Kiyokawa E et al (2005) Spatial and functional heterogeneity of sphingolipid-rich membrane domains. J Biol Chem 280(25):24072–24084
34. Kidani Y et al (2012) Differential localization of sphingomyelin synthase isoforms in neurons regulates sphingomyelin cluster formation. Biochem Biophys Res Commun 417(3):1014–1017
35. Yamaji A et al (1998) Lysenin, a novel sphingomyelin-specific binding protein. J Biol Chem 273(9):5300–5306
36. Kobayashi H, Suzuki H, Ohta N (2006) Exfoliation of the epidermal cells and defecation by amphibian larvae in response to coelomic fluid and lysenin from the earthworm *Eisenia foetida*. Biomed Res 27(4):169–181
37. Bittman R, Fischkoff SA (1972) Fluorescence studies of the binding of the polyene antibiotics filipin 3, amphotericin B, nystatin, and lagosin to cholesterol. Proc Natl Acad Sci U S A 69 (12):3795–3799
38. Orci L et al (1981) Heterogeneous distribution of filipin–cholesterol complexes across the cisternae of the Golgi apparatus. Proc Natl Acad Sci U S A 78(1):293–297
39. Ohno-Iwashita Y et al (2004) Perfringolysin O, a cholesterol-binding cytolysin, as a probe for lipid rafts. Anaerobe 10(2):125–134
40. Hayashi M et al (2006) Detection of cholesterol-rich microdomains in the inner leaflet of the plasma membrane. Biochem Biophys Res Commun 351(3):713–718
41. Schroeder F et al (1991) Transmembrane distribution of sterol in the human erythrocyte. Biochim Biophys Acta 1066(2):183–192
42. Mukherjee S et al (1998) Cholesterol distribution in living cells: fluorescence imaging using dehydroergosterol as a fluorescent cholesterol analog. Biophys J 75(4):1915–1925
43. Wustner D (2007) Plasma membrane sterol distribution resembles the surface topography of living cells. Mol Biol Cell 18(1):211–228

44. Tasset C et al (1992) Comparison of nephrotoxicities of different polyoxyethyleneglycol formulations of amphotericin B in rats. Antimicrob Agents Chemother 36(7):1525–1531
45. Nagy E et al (2007) Hyperfluidization-coupled membrane microdomain reorganization is linked to activation of the heat shock response in a murine melanoma cell line. Proc Natl Acad Sci U S A 104(19):7945–7950
46. Sato SB et al (2004) Distribution and transport of cholesterol-rich membrane domains monitored by a membrane-impermeant fluorescent polyethylene glycol-derivatized cholesterol. J Biol Chem 279(22):23790–23796
47. Pagano RE et al (1991) A novel fluorescent ceramide analogue for studying membrane traffic in animal cells: accumulation at the Golgi apparatus results in altered spectral properties of the sphingolipid precursor. J Cell Biol 113(6):1267–1279
48. Marks DL, Bittman R, Pagano RE (2008) Use of Bodipy-labeled sphingolipid and cholesterol analogs to examine membrane microdomains in cells. Histochem Cell Biol 130(5):819–832
49. D'Auria L et al (2011) Segregation of fluorescent membrane lipids into distinct micrometric domains: evidence for phase compartmentation of natural lipids? PLoS One 6(2):e17021
50. Greaves J, Chamberlain LH (2011) Differential palmitoylation regulates intracellular patterning of SNAP25. J Cell Sci 124(Pt 8):1351–1360
51. Lajoie P, Nabi IR (2007) Regulation of raft-dependent endocytosis. J Cell Mol Med 11 (4):644–653
52. Anderson RG (1993) Plasmalemmal caveolae and GPI-anchored membrane proteins. Curr Opin Cell Biol 5(4):647–652
53. Rothberg KG et al (1992) Caveolin, a protein component of caveolae membrane coats. Cell 68 (4):673–682
54. Scherer PE et al (1997) Cell-type and tissue-specific expression of caveolin-2. Caveolins 1 and 2 co-localize and form a stable hetero-oligomeric complex in vivo. J Biol Chem 272 (46):29337–29346
55. Tang Z et al (1996) Molecular cloning of caveolin-3, a novel member of the caveolin gene family expressed predominantly in muscle. J Biol Chem 271(4):2255–2261
56. Parton RG (1996) Caveolae and caveolins. Curr Opin Cell Biol 8(4):542–548
57. Mundy DI et al (2002) Dual control of caveolar membrane traffic by microtubules and the actin cytoskeleton. J Cell Sci 115(Pt 22):4327–4339
58. Glebov OO, Bright NA, Nichols BJ (2006) Flotillin-1 defines a clathrin-independent endocytic pathway in mammalian cells. Nat Cell Biol 8(1):46–54
59. Frick M et al (2007) Coassembly of flotillins induces formation of membrane microdomains, membrane curvature, and vesicle budding. Curr Biol 17(13):1151–1156
60. Riento K et al (2009) Endocytosis of flotillin-1 and flotillin-2 is regulated by Fyn kinase. J Cell Sci 122(Pt 7):912–918
61. Blanchet MH et al (2008) Cripto recruits Furin and PACE4 and controls Nodal trafficking during proteolytic maturation. EMBO J 27(19):2580–2591
62. Weber G, Farris FJ (1979) Synthesis and spectral properties of a hydrophobic fluorescent probe: 6-propionyl-2-(dimethylamino)naphthalene. Biochemistry 18(14):3075–3078
63. Bagatolli LA et al (1999) A model for the interaction of 6-lauroyl-2-(N, N-dimethylamino) naphthalene with lipid environments: implications for spectral properties. Photochem Photobiol 70(4):557–564
64. Parasassi T et al (1990) Phase fluctuation in phospholipid membranes revealed by Laurdan fluorescence. Biophys J 57(6):1179–1186
65. Parasassi T et al (1991) Quantitation of lipid phases in phospholipid vesicles by the generalized polarization of Laurdan fluorescence. Biophys J 60(1):179–189
66. Buffone MG et al (2009) High cholesterol content and decreased membrane fluidity in human spermatozoa are associated with protein tyrosine phosphorylation and functional deficiencies. J Androl 30(5):552–558
67. Kaiser HJ et al (2011) Molecular convergence of bacterial and eukaryotic surface order. J Biol Chem 286(47):40631–40637

68. Gaus K et al (2003) Visualizing lipid structure and raft domains in living cells with two-photon microscopy. Proc Natl Acad Sci U S A 100(26):15554–15559
69. Khan NA et al (2011) Stability of fatty acids during wilting of perennial ryegrass (*Lolium perenne* L.): effect of bruising and environmental conditions. J Sci Food Agric 91 (9):1659–1665
70. Owen DM et al (2010) Imaging membrane lipid order in whole, living vertebrate organisms. Biophys J 99(1):L7–L9
71. Wheeler G, Tyler KM (2011) Widefield microscopy for live imaging of lipid domains and membrane dynamics. Biochim Biophys Acta 1808(3):634–641
72. Hansen JS, Helix-Nielsen C (2011) An epifluorescence microscopy method for generalized polarization imaging. Biochem Biophys Res Commun 415(4):686–690
73. Sanchez SA, Tricerri MA, Gratton E (2007) Interaction of high density lipoprotein particles with membranes containing cholesterol. J Lipid Res 48(8):1689–1700
74. Weber P, Wagner M, Schneckenburger H (2010) Fluorescence imaging of membrane dynamics in living cells. J Biomed Opt 15(4):046017
75. Toyoda T et al (2009) Thermo-sensitive response based on the membrane fluidity adaptation in *Paramecium multimicronucleatum*. J Exp Biol 212(17):2767–2772
76. Sitrin RG et al (2010) Migrating human neutrophils exhibit dynamic spatiotemporal variation in membrane lipid organization. Am J Respir Cell Mol Biol 43(4):498–506
77. Parasassi T et al (1997) Two-photon fluorescence microscopy of laurdan generalized polarization domains in model and natural membranes. Biophys J 72(6):2413–2429
78. Kim HM et al (2007) A two-photon fluorescent probe for lipid raft imaging: C-laurdan. Chembiochem 8(5):553–559
79. Klemm RW et al (2009) Segregation of sphingolipids and sterols during formation of secretory vesicles at the trans-Golgi network. J Cell Biol 185(4):601–612
80. Jin L et al (2005) Cholesterol-enriched lipid domains can be visualized by di-4-ANEPPDHQ with linear and nonlinear optics. Biophys J 89(1):L04–L06
81. Jin L et al (2006) Characterization and application of a new optical probe for membrane lipid domains. Biophys J 90(7):2563–2575
82. Dinic J et al (2011) Laurdan and di-4-ANEPPDHQ do not respond to membrane-inserted peptides and are good probes for lipid packing. Biochim Biophys Acta 1808(1):298–306
83. Owen DM, Gaus K (2010) Optimized time-gated generalized polarization imaging of Laurdan and di-4-ANEPPDHQ for membrane order image contrast enhancement. Microsc Res Tech 73 (6):618–622
84. Llopis J et al (2000) Ligand-dependent interactions of coactivators steroid receptor coactivator-1 and peroxisome proliferator-activated receptor binding protein with nuclear hormone receptors can be imaged in live cells and are required for transcription. Proc Natl Acad Sci U S A 97(8):4363–4368
85. Miyawaki A (2011) Development of probes for cellular functions using fluorescent proteins and fluorescence resonance energy transfer. Annu Rev Biochem 80:357–373
86. Miyawaki A, Tsien RY (2000) Monitoring protein conformations and interactions by fluorescence resonance energy transfer between mutants of green fluorescent protein. Methods Enzymol 327:472–500
87. Nagai T et al (2002) A variant of yellow fluorescent protein with fast and efficient maturation for cell-biological applications. Nat Biotechnol 20(1):87–90
88. Griesbeck O et al (2001) Reducing the environmental sensitivity of yellow fluorescent protein. Mechanism and applications. J Biol Chem 276(31):29188–29194
89. Rao M, Mayor S (2005) Use of Forster's resonance energy transfer microscopy to study lipid rafts. Biochim Biophys Acta 1746(3):221–233
90. Ariola FS et al (2009) Membrane fluidity and lipid order in ternary giant unilamellar vesicles using a new bodipy-cholesterol derivative. Biophys J 96(7):2696–2708
91. Bader AN et al (2009) Homo-FRET imaging enables quantification of protein cluster sizes with subcellular resolution. Biophys J 97(9):2613–2622

92. Sharma SD et al (2004) Radiochromic film measurement of anisotropy function for high-dose-rate Ir-192 brachytherapy source. Phys Med Biol 49(17):4065–4072
93. Hoppe AD et al (2008) Three-dimensional FRET reconstruction microscopy for analysis of dynamic molecular interactions in live cells. Biophys J 95(1):400–418
94. Verveer PJ, Squire A, Bastiaens PI (2000) Global analysis of fluorescence lifetime imaging microscopy data. Biophys J 78(4):2127–2137
95. de Almeida RF, Loura LM, Prieto M (2009) Membrane lipid domains and rafts: current applications of fluorescence lifetime spectroscopy and imaging. Chem Phys Lipids 157 (2):61–77
96. Owen DM et al (2006) Fluorescence lifetime imaging provides enhanced contrast when imaging the phase-sensitive dye di-4-ANEPPDHQ in model membranes and live cells. Biophys J 90(11):L80–L82